Ocean Heat Transport crossing AR7W in the Labrador Sea

Melinda M. Hall and Daniel J. Torres, Woods Hole Oceanographic Institution, Woods Hole, MA

Introduction

Fundamental to understanding the world's climate system and its variability is an understanding of the ocean's participation in redistributing heat meridionally through oceanic transport and sea-air buoyancy fluxes. Deep convective processes occurring in the subpolar seas of the North Atlantic result in ventilation of the intermediate and deep water masses of the world ocean, and therefore fundamentally contribute to the meridional overturning circulation. In this presentation we expand and build on work that has been presented previously, examining the velocity field determined from lowered ADCP data collected along AR7W in the Labrador Sea between 1995 and 2001. Despite obvious and significant changes in the circulation pattern from year to year, a well-organized velocity field emerges when we combine the different data sets to create a composite velocity field. Incorporating hydrographic data (provided by the Ocean Sciences Division at BIO in Dartmouth, Nova Scotia) allows us to estimate the poleward heat flux crossing this section.

1a

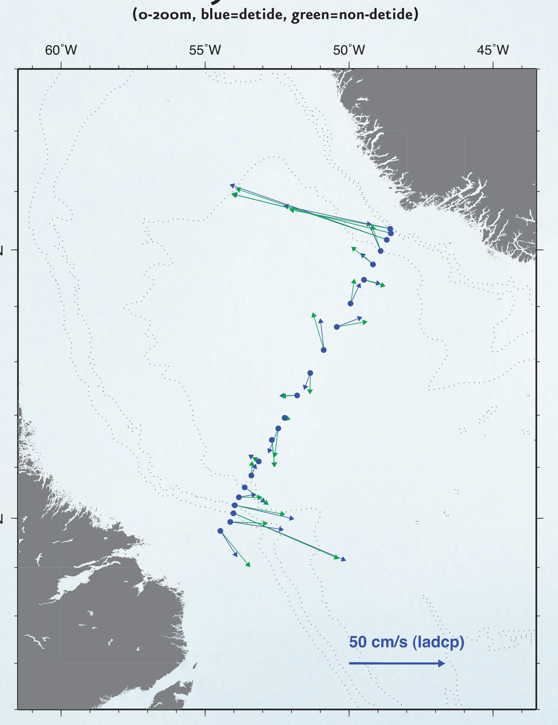

Figure 1a shows the location of the AR7W line crossing the Labrador Sea from southwest to northeast. Hydrographic and ADCP (lowered and vessel-mounted) data are collected annually at 28 nominal station sites, and have been processed following Firing and Gordon (1990) and Fischer and Visbeck (1993).

Lowered ADCP observations include both geostrophic and ageostrophic velocity contributions. It is impossible to filter out all the ageostrophic contributions (in the interest of approximating the geostrophically balanced flow), but we can use a regional tidal model to remove the tides from the LADCP data (Egbert and Erofeeva, 2002). This model incorporates satellite altimetry observations to predict the barotropic tidal velocity for each station location at the time it was occupied: for example, Figures 1b and 1c show the tidal velocities (U and V) predicted by the model over a time span covering the May, 1996, occupation of AR7W, as well as the tidal ellipses: the blue dots in all plots indicate the date and time of station 26 (1b), up on the shelf, and 36 (1c), in the center of the basin. The tidal ellipse in the center of the basin is nearly flat, and aligned with the basin's axis; that over the shelf is much rounder. Station 26 was occupied near a tidal extremum, while station 36 occurred near a node. Figure 1a demonstrates the relative importance of the tidal component by comparing depth-averaged LADCP velocities between 0 and 200 m before (green) and after (blue) removing the tides.

1b **Tidal Model Time Series at Single Station**

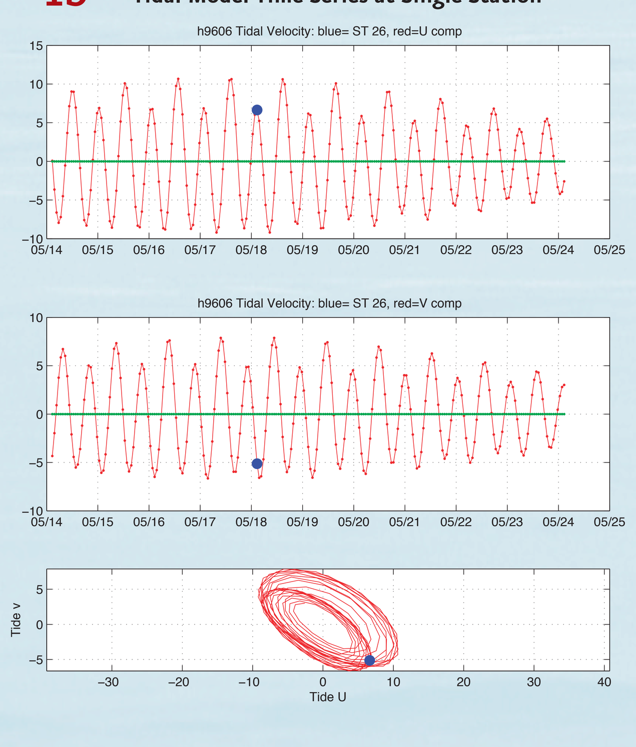

1c **Tidal Model Time Series at Single Station**

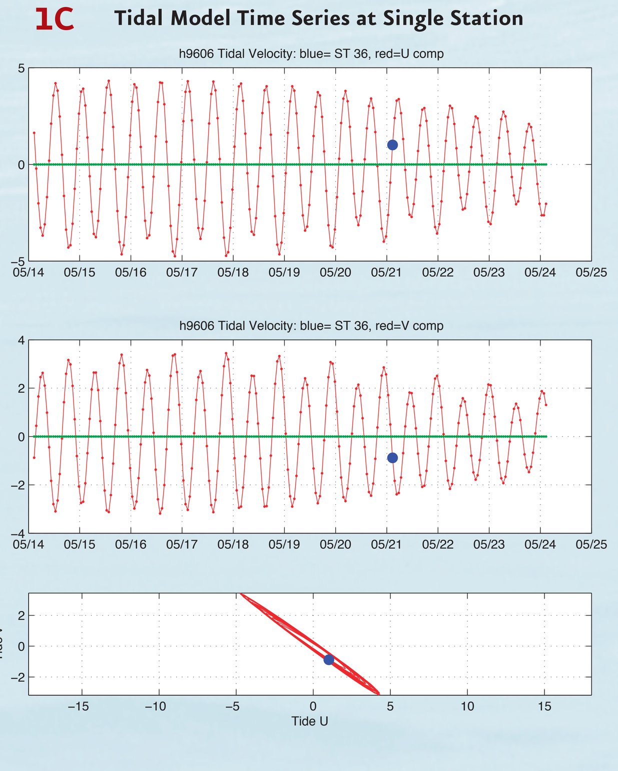

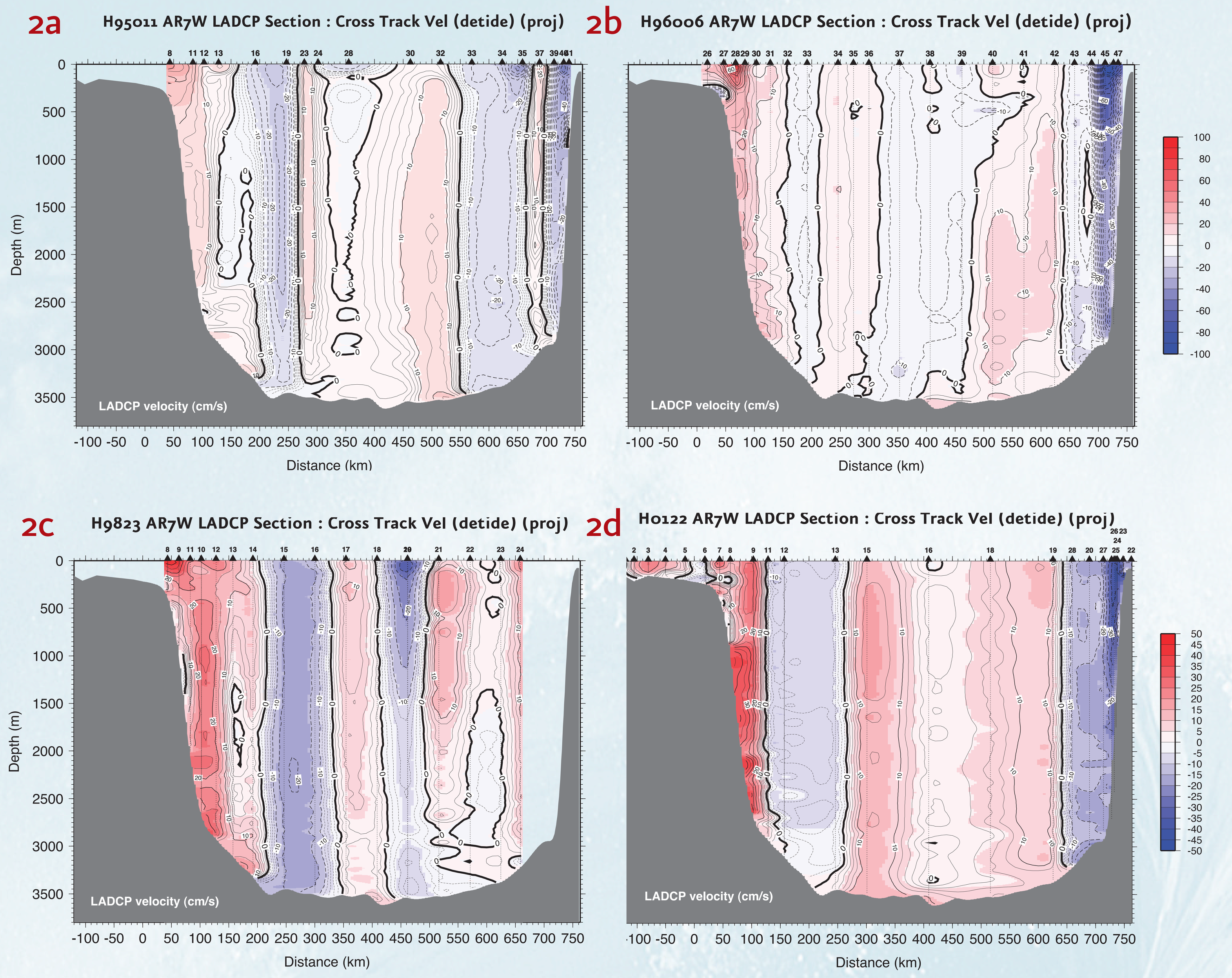

Since we are interested in evaluating mass and property transports crossing the AR7W line, we have rotated the velocities into a coordinate system with axes along and orthogonal to the AR7W line (specifically, the rotation angle is 30 degrees in the clockwise direction). Although an effort is made to occupy the ideal AR7W station sites every year, slight differences naturally occur (depending on weather, currents, etc.); to facilitate comparisons between different years, we have also projected the observations to lie along a straight line: 0 km corresponds to 54.62°N, 54.65°W; 760 km is 60.56°N, 48.32°W. The cross-track velocities are shown in Figure 2 and have had the tidal components removed. The sections were occupied in June, 1995 (H95011); May, 1996 (H96006); June-July, 1998 (H9823); and June, 2001 (H0122). Note that the color scale varies for each section.

All 4 crossings clearly show the equatorward boundary current on the western end and the poleward boundary current on the eastern end (except for 1998, when the cruise was unable to occupy the easternmost sites). In 1995, the deep velocity maximum on the western end extends much farther offshore than in other years, perhaps a result of topographic Rossby waves. The interior flow is largely barotropic, with alternating bands of transport that vary in strength, position and extent from year to year. We have noted in past work that geostrophic velocities alone are inadequate to capture this part of the flow field, due to its barotropic nature. Geostrophic and LADCP velocity shear are generally in good agreement in regions of stronger shear (not shown).

3a **AR7W 4 Year Composite Cross Track Vel (detide) (proj)**

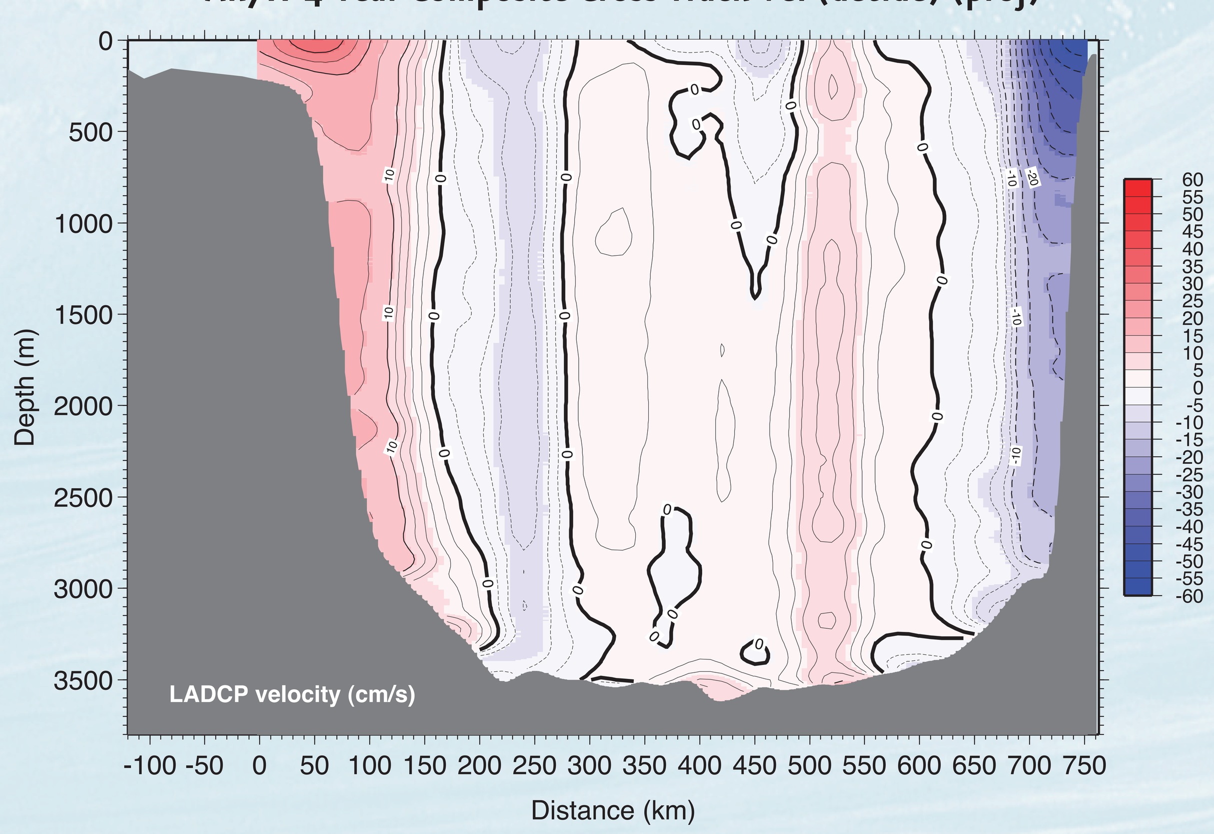

3b **AR7W 4 Year Composite Cross Track Vel STD (detide) (proj)**

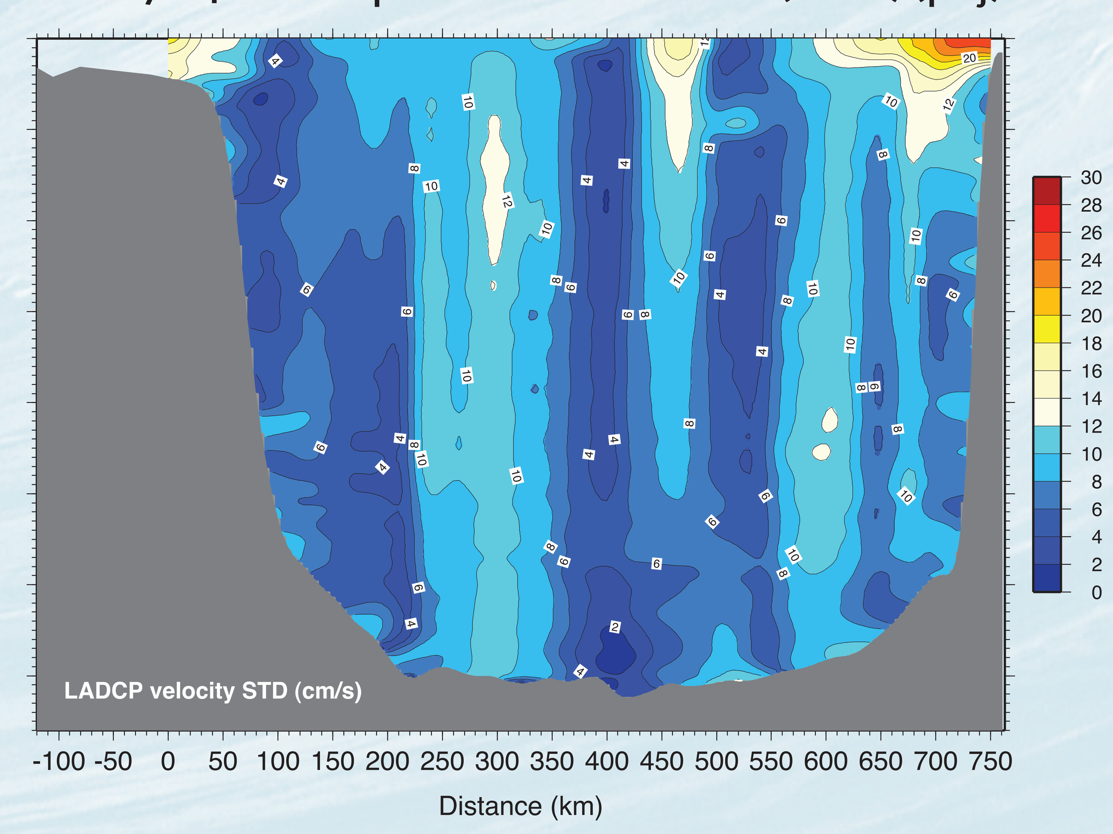

To form a composite velocity section, we have objectively mapped the individual sections onto a uniform grid (with Gaussian weighting parameters of 30 km and 50 m in the horizontal and vertical, respectively), and then averaged them. The result is shown in Figure 3, along with the standard deviation. (Since the western shelf area was occupied only in 2001, we have omitted those values from this composite.) Over much of the section, the standard deviation ranges from 5-10 cm/sec, while it is strongest where the velocities are strongest, in the surface portion of the boundary currents.

The structure of our composite velocity resembles that of Pickart and Spall's (2007, hereafter PS2007) composite velocity, which was based only on hydrographic and float data. The main difference is that, for our composite, observed velocities tend to be stronger throughout; otherwise, the top-to-bottom transitions from poleward to equatorward flow (and vice versa) occur at nearly the same location. Furthermore, mass transport crossing AR7W is balanced to within 2 Sv in our composite. (Both the similarity to PS2007 and the nearly balanced transport are probably coincidental, however, since PS2007 found that a stable mean circulation was achieved only when including more than about 8 realizations of the velocity field in their analysis.)

For our composite section, the western boundary current transports about 30 Sv southeastward, inshore of the 3100 m isobath; and the eastern boundary current transports about 40 Sv northwestward, 33 Sv of which occurs inshore of the 3100 m isobath. For comparison, PS2007 diagnosed a boundary current "throughput" of 28.5 Sv.

4 **Cumulative Transport Along AR7W**

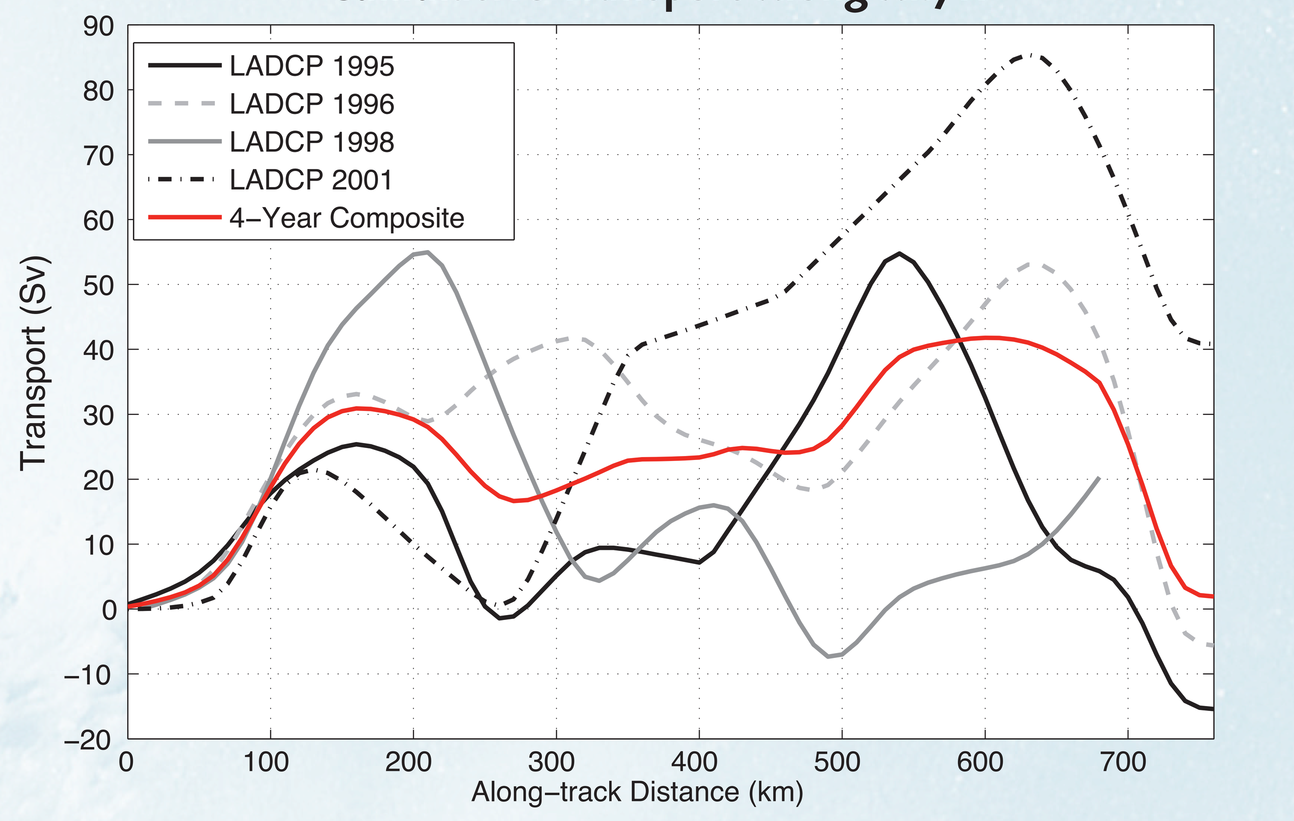

The cumulative transport, integrated eastward from the western end of AR7W, is shown in Figure 4 for all four years as well as for the composite section. Transport in the western boundary current ranges from about 20 Sv (2001) to over 50 Sv (1995); the eastern boundary current is more difficult to evaluate, since 1998 data are missing and in the 1995 section it is unclear whether the offshore flow is actually part of the boundary current (we should be able to sort this out eventually using the hydrographic data). The variability between sections is smoothed out in the composite. Note that the mass is nearly balanced across the section, facilitating our heat flux calculation, which depends on net mass transport being zero.

5

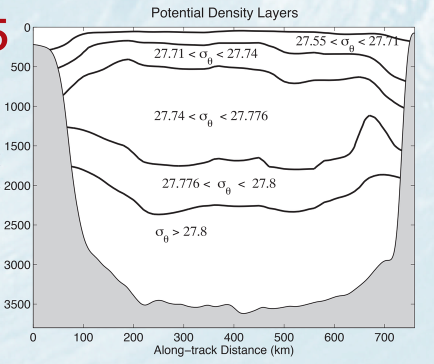

One goal of our work is to determine how much heat the ocean transports poleward across AR7W. Because heat flux is well-defined only for a mass-conserving system, simple constraints on mass conservation are required to determine it. In addition to overall mass transport being negligible, we also expect transport in density layers to be conserved within a certain range, particularly (following PS2007) for $\sigma_\theta > 27.8$, the density range of overflow waters passing through the Labrador Sea relatively unchanged. To achieve this, we have applied a simple inverse model conserving mass within prescribed ranges for the 6 density layers shown in Figure 5. This model can be applied to the composite velocity section deduced from the LADCP alone, using a composite hydrographic section for temperature, density, etc., or to geostrophic velocities that have been referenced to the LADCP profiles for individual years.

For the former, our model yields a slight mass divergence for the thin surface layers; convergence in the next two layers; and some divergence in the lowest layers (the deepest conserves mass within half a Sv), consistent with PS2007, Figure 9. The velocity adjustments have a standard deviation of 2.4 cm/sec, with the largest values (8 cm/sec) occurring in the boundary currents. The heat flux associated with this circulation is 119 TW (1 Tera Watt = 10^{12} Watts), of which a negligible amount occurs in the deepest layer. This is more than 3 times as large as that found by PS2007 (37.6 TW), even though their circulation was meant to represent the spring season, as does ours.

To investigate further, we have made similar calculations for the three individual occupations that covered the entire section. The resulting heat fluxes range from 50.4 TW in 1995, for which we had only 18 useful LADCP stations; to 126 TW for 1996, which had the best coverage; in 2001, an intermediate value of 92.3 TW was obtained. In all cases, negligible flux occurs in the deepest layer. Finally, if we apply the same inverse model to bottom-relative geostrophic velocity alone (ignoring the LADCP data), much weaker heat flux results: for the 1996 section, we obtain just 41.5 TW, compared to 126 TW when we use the LADCP velocity as well. Clearly, inclusion of absolute velocity from the LADCP captures an important aspect of the circulation. We hypothesize that this accounts for the difference between our heat flux results and those of PS2007.

Acknowledgments:

We would like to thank the many individuals at Bedford Institute of Oceanography whose cooperation has made the collection of this dataset possible. We especially thank Igor Yashayaev, Allyn Clarke, John Lazier, and John Loder.

This material is based upon work supported by the National Science Foundation under Grant No. 0622640.

References:

Egbert, G.D., and S.Y. Erofeeva, 2002: Efficient inverse modeling of barotropic ocean tides, *J. Atmos. Oceanic Technol.*, 19(2), 183-204.

Firing, E., and L. Gordon, 1990. Deep ocean acoustic doppler current profiling. *Proc. IEEE Fourth Working Conf. on Current Measurements*, Clinton, MD, Current Measurement Technology Committee of the Ocean Engineering Society, 192–201.

Fischer, J., and M. Visbeck, 1993: Deep velocity profiling with self contained ADCPs. *Journal of Atmospheric and Oceanic Technology*, 10, 764-773.

Hall, M. M., and D. J. Torres, 2008: Absolute velocity in the Labrador Sea: ADCP Observations along AR7W. Poster presented at Ocean Sciences Meeting, Orlando, FL, March 2008. Online at http://www.whoi.edu/page.do?pid=24638.

Pickart, R. S. and M. A. Spall, 2007: Impact of Labrador Sea Convection on the North Atlantic Meridional Overturning Circulation. *J. Phys. Oceanogr.*, 37, 2207-2227.